

Characterization of a Dermal Derived Malignant Mesenchymal Tumor Arising in Ultraviolet Irradiated Mice

Robert G. Phelps, Lori E. Bernstein, Noam Harpaz, Ronald E. Gordon, Frederick A. Cruickshank, and Elaine Schwartz

From the Departments of Dermatology and Pathology, The Mount Sinai School of Medicine, New York, New York

Skh/hr-1 hairless albino mice were irradiated with photocarcinogenic dosages of ultraviolet light for periods of 30 weeks or longer. A high proportion of mice developed pleomorphic spindle cell tumors and epidermal neoplasms of various types. These spindle cell tumors were studied by immunofluorescence and immunoperoxidase techniques and by electron microscopy. Freshly isolated tumor cells were grown in tissue culture. Immunocytochemical analysis showed varying expression of markers of mesenchymal differentiation: vimentin, procollagens I and III, type I collagen, and lysozyme. Electron microscopy showed spindled and cuboidal cells with abundant endoplasmic reticulum, filopodia, and lysosomes, but no intercellular connections. The cells grown in vitro were cuboidal and stellate and also showed mesenchymal differentiation by electron microscopy. These results are perhaps similar to those described for a human atypically produced fibrohistiocytic neoplasm, atypical fibroxanthoma, and this system may provide a useful model of ultraviolet-induced dermal neoplasia. (Am J Pathol 1989, 135:149-159)

Atypical fibroxanthoma is a rare low grade malignant neoplasm that occurs primarily on the head and neck of the elderly, and is believed to occur as a consequence of actinic damage.¹⁻⁶ For many years its precise histogenesis was controversial. Many authors considered it representative of a spectrum of lesions, including poorly differentiated squamous cell carcinomas,⁷ malignant melanoma, and various types of mesenchymal tumors. Only more recent electron microscopic and immunocytochemical methods have clearly defined it as an entity *sui generis*.⁸⁻¹⁵

The difficulty in defining and accepting atypical fibroxanthoma stemmed from two sources. First, ultraviolet (UV) irradiation (principally in the UVB range) is linked primarily to epidermal neoplasia.¹⁶ As UVB barely penetrates the epidermis and is the primary photocarcinogenic wavelength region,¹⁷ dermal neoplasia would be less expected. Second, there are numerous experimental models for epidermal photocarcinogenesis, but there is no clearly defined experimental model with which to study dermal photocarcinogenesis.

Pleomorphic spindle cell tumors induced in hairless albino mice (Skh/hr-1) by UV irradiation showed features similar to human atypical fibroxanthoma. The purpose of this study was to demonstrate that these spindle cell tumors were dermally derived, and that the tumors resembled human atypical fibroxanthoma.

To accomplish this, the tumors were studied temporally, to determine early histogenetic origins. Furthermore, at each developmental stage the tumors were studied by immunocytochemical, electron microscopic, or tissue culture techniques to correlate the morphologic observations with the presumed histogenesis.

Materials and Methods

Irradiation

Ten-week old hairless albino mice (Skh/hr-1) were subjected to intense ultraviolet irradiation according to the following schedule.

Three times a week, the mice were placed in special stainless steel cages, 45 cm below a bank of six Westinghouse FS20 sunlamps (Dermacontrol, Dolton, IL). For the

This work was supported in part by NIH grant #AR36101.

This work was presented in part at the 48th and 49th Annual Meetings of the Society for Investigative Dermatology at San Diego, California and Washington, DC, respectively, May 4-6, 1987, April 27-30, 1988.

Accepted for publication March 30, 1989.

Address reprint requests to Dr. Robert G. Phelps, Director, Dermatopathology Division, Departments of Dermatology and Pathology, Annenberg 24-62, The Mount Sinai Medical Center, One Gustave L. Levy Place, New York, NY 10029.

first 4 weeks, the mice were exposed 10 minutes each day (0.1 J/cm² for UVA and UVB). The exposure times were then increased by 5 minutes every 2 weeks to 30 minutes by the 10th week (0.3 J/cm² UVA and UVB). The exposure times were then maintained until the mice were sacrificed.

Starting at 20 weeks, the mice were inspected at weekly intervals for the presence of epidermal thickening, keratoses, or epidermal tumors. Those mice with morphologically atypical lesions, eg, lesions that were round and flesh colored, were separated. Once these lesions became large enough to analyze, the mice were sacrificed by cervical dislocation. Selected mice were also subjected to extensive postmortem examinations.

Routine Histology

Histologic slides of 8 μ m thickness were prepared from 10% buffered formalin-fixed and paraffin-embedded tissue and stained with hematoxylin and eosin (H&E), Verhoeff von Gieson (EVG), trichrome, reticulin, and alcian blue stains by standard methods.

Sources of Antibodies

For immunoperoxidase studies, rabbit anti-human epidermal keratin and anti-"wide spectrum" keratin (Dako Corporation, Santa Barbara, CA) were used. The former is directed against higher molecular weight keratins derived from human plantar callus,¹⁸ and the latter against high and low molecular weight species derived from bovine muzzle.¹⁹

Rabbit anti-human lysozyme, anti-human α_1 -antitrypsin, and anti-bovine S-100 protein were also obtained from Dako Corporation. Optimal concentrations of primary antibodies were determined by titration with sections of suitable positive control tissues.

Antibodies used for immunofluorescence studies included guinea pig anti-bovine keratin, rabbit anti-murine vimentin, anti-bovine collagen I, anti-procollagens I and III, anti-mouse type IV-7S collagen, and anti-mouse nidogen.

Rabbit anti-murine vimentin was prepared from extracts of fibroblast cytoskeleton²⁰ and was a gift from Dr. D. Bucher (The Mt. Sinai Medical Center, NY). Guinea pig anti-bovine keratin was obtained from ICN immunobiologicals (Costa Mesa, CA), and was directed against bovine hoof keratin.¹⁹

Antibodies against bovine collagen I and against the aminopeptides of bovine procollagens I and III were affinity purified and freed of crossreacting antibodies according to previously published methods.²¹ The Englebreth-Holm-Swarm sarcoma provided basal lamina anti-

gens used to prepare antibodies against nidogen and the 7S domain of type IV collagen.^{22,23} All anti-collagen and basal lamina antibodies were kindly provided by Dr. R. Timpl, Max Planck Institute for Biochemistry, West Germany.

Immunoperoxidase

For immunoperoxidase studies, the avidin-biotin peroxidase method²⁴ was used. Saponin, porcine stomach pepsin, and diaminobenzidine were obtained from Sigma Chemical Company, St. Louis, MO and avidin-biotin complex (Vectastain) from Vector Laboratories, Burlingame, CA. Six micron thick sections of 10% buffered formalin-fixed, paraffin-embedded tissue were heated at 60 C overnight, deparaffinized with xylene, rehydrated through graded alcohols and water, and treated with 1% hydrogen peroxide for 15 minutes at room temperature to eliminate endogenous peroxidase activity. Sections were then predigested with either 0.1% pepsin in 0.01 N HCl (keratins) or 0.05% saponin in distilled water (other antigens) for 30 minutes at room temperature. Sections were incubated in 10% normal horse serum in phosphate-buffered saline (PBS) to block nonspecific antibody binding and incubated with primary antibody or normal rabbit serum (negative controls), both 1:500 in PBS, overnight at 4 C. After washing with PBS, the sections were incubated with biotinylated goat anti-rabbit antiserum (1:200 in PBS) for 30 minutes at room temperature. After additional washing, the sections were incubated with avidin-biotin complex for 30 minutes at room temperature and washed; the reaction product developed with a fresh solution of 0.02% diaminobenzidine in PBS containing 0.5% Triton X-100 (Sigma Chemical Co., St. Louis, MO), for 1 to 5 minutes. The sections were washed with distilled water, counterstained with hematoxylin, dehydrated in graded alcohols and xylene, and mounted. Suitable parallel positive and negative controls were included with each determination.

Immunofluorescence

Fresh or frozen tissue was placed in Tissue-Tek II (Miles Laboratories Elkhart, IN) embedded and cooled to -20 C. Frozen sections were cut at 6 μ m in a cryotome (American Optical, Buffalo, NY).

Tissue sections were fixed for 5 minutes in cold acetone, washed, and predigested with 2% crude testicular hyaluronidase for 30 minutes at room temperature. After washes with PBS, the primary antibody was applied overnight at 4 C. Optimal dilutions were determined with known positive control tissues. The sections were washed with PBS, reacted with fluorescein-conjugated

secondary antibody, and washed again; fluorescence was viewed with a Nikon Fluophot photomicroscope (Garden City, NY). For controls, comparable dilutions of normal rabbit serum or normal rabbit immunoglobulin were used in place of primary antibodies.

Tissue Culture

Fresh tumor tissue was isolated under sterile conditions from recently sacrificed hairless mice. The tissue was finely minced in a petri dish containing Ham's F10 with 10% fetal bovine serum. After adhesion of individual explants (within 48 to 96 hours), the medium was changed three times a week for periods up to 3 weeks.

Electron Microscopy

Tumor tissue was fixed in 3% glutaraldehyde in cacodylate buffer, osmicated, dehydrated through graded alcohols and propylene oxide, and embedded in LX112 resin. Thin sections were cut in an ultramicrotome LKB4 (Bromma, Sweden) and viewed in an electron microscope JEM 100 CX (Jeol, Tokyo, Japan).

Tissue culture plates were fixed, osmicated, dehydrated, and embedded *in situ* in a similar fashion, with the omission of the propylene oxide step.²⁵ Thin sections were taken perpendicular to the monolayer.

Results

Skh/hr-1 hairless albino mice were irradiated with high doses of UV irradiation in groups of five to ten. By 20 weeks, virtually all the mice showed evidence of UV-induced damage. The dorsal skin was thickened, wrinkled, and leathery.

Histopathologic examination at 20 weeks showed an epidermis with uniform psoriasiform hyperplasia and a compact horn, but without evidence of dysplasia. The dermis showed an increase in mast cells and an inflammatory reaction to ruptured follicular cysts. EVG stains showed hyperplasia of elastic fibers.

After 25 to 30 weeks, virtually all mice showed evidence of early epidermal neoplasia. In addition to the thickened skin, there were areas of fine scaling in small 1 mm to 2 mm foci, or larger, approximately 1 cm scales. These gradually evolved into small papillary excrescences that merged into larger exophytic papillomatous lesions.

Histologic examination showed a wide spectrum of dysplastic lesions. Flattened scaly lesions showed foci of epidermal dysplasia or full-thickness dysplasia sugges-

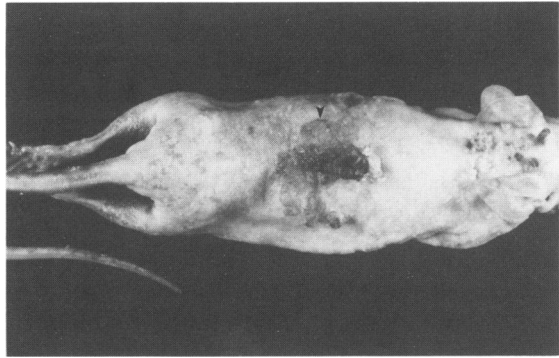


Figure 1. Hairless albino mouse (*Skh/br-1*) after 34 weeks of UV irradiation to the dorsum. In addition to the diffuse crusting and scaling, there is a small, dome-shaped, 0.5 to 1 cm, flesh colored, dermal nodule (arrowhead).

tive of an actinic keratosis or Bowenoid actinic keratosis. Larger lesions showed dysplastic squamous papillomas, suggestive of hypertrophic actinoid keratoses. Many of these larger lesions showed invasion of atypical keratinocytes into dermis consistent with superficial squamous cell carcinoma.

After 30 weeks, these papillomatous lesions continued to grow, forming large, often ulcerated, chalky, exophytic masses that covered the entire dorsum. In some mice, however, a second population of tumors emerged.

Adjacent to the bulky grumous tumors, small flesh colored morphologically distinctive dermal nodules appeared (Figure 1). They had few surface alterations, grew progressively by an apparent centrifugal growth, and pushed the epidermis upward while expanding the dermis. As the nodules continued to grow, their spherical



Figure 2. Hairless albino mouse (*Skh/br-1*) after 37 weeks of UV irradiation. Adjacent to a thickened, crusted dorsum is a large exophytic, ulcerated flesh colored, sarcomatous nodule.

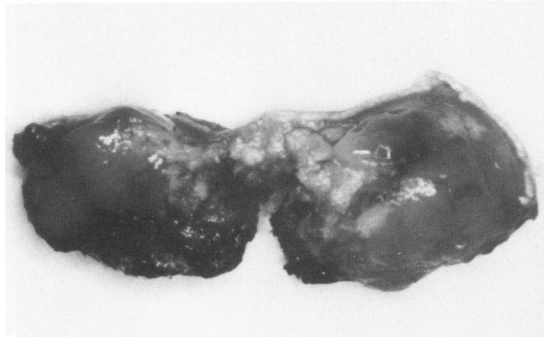


Figure 3. Cross section of flesh colored nodule from Figure 2.

contour contrasted sharply with the adjacent epithelial keratotic lesions (Figure 2). Grossly, the nodules were homogeneous and flesh colored (Figure 3).

Light microscopy of early lesions showed poorly delineated dermal nodules of atypical spindle cells and giant cells. These nodules were poorly demarcated, infiltrated into deep dermis and skeletal muscles, and pushed the overlying epidermis upward. As they continued to grow, the overlying epidermis became atrophic or ulcerated, and the tumors often showed multiple foci of necrosis. In these later lesions, adjacent epidermis invariably showed dysplasia, carcinoma *in situ*, or overt invasive squamous carcinoma. Despite the apparent juxtaposition of spindle cell tumors and epidermal neoplasia, an unequivocal transition from keratinocytes could not be demonstrated (Figure 4).

Cytologically, these tumors were quite varied. In most areas, there were poorly demarcated, randomly arrayed fascicles of plump spindle cells (Figures 5 and 6). They did not appear to form any clear organoid pattern and merged imperceptibly with clusters of atypical cuboidal cells (Figure 7). Numerous mitotic figures and frequent areas of necrosis were present (Figure 5).

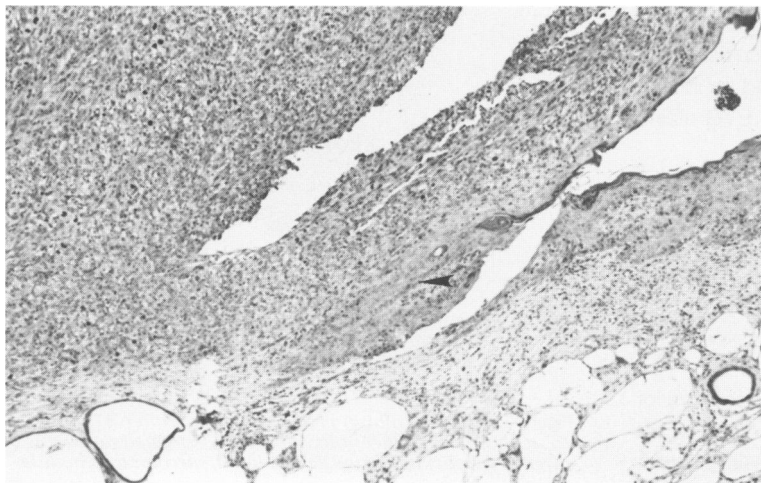


Figure 4. Spindle cell tumor at 37 weeks. Overlying and in the dermis there is an irregularly demarcated, atypical spindle cell neoplasm. The peripheral epidermis is acanthotic and atypical but fails to merge with the tumor (arrowhead) (H&E, $\times 80$).

With sufficient exposure time, approximately 25% of mice developed these spindle cell tumors, whereas all mice developed epidermal neoplasia. Postmortem examinations of 5 mice with samplings of major viscera and lymphatics failed to disclose evidence of metastases of squamous cell carcinomas or sarcomas.

Immunoperoxidase Studies

Both types of antikeratin antibody showed identical patterns of staining. Adjacent normal epidermis, dysplastic epidermis, and squamous carcinoma showed intense intracytoplasmic staining of keratinocytes, whereas the spindle cells were invariably negative (Figure 8). Horn pearls of the carcinomas and the follicular cysts of the hairless mice stained as well.

Intracytoplasmic lysozyme was detected in occasional cuboidal histiocytic type cells (Figure 7), whereas the staining of spindle cells was weak or absent. Alpha-1-antitrypsin failed to show significant staining. Anti-S-100 protein stained only occasional dermal and epidermal dendritic cells, which were interpreted as Langerhans cells (Figure 9).

Immunofluorescence

Antivimentin antibodies showed intense intracytoplasmic staining of all cells, the cytosol contrasting against the unstained nucleus (Figure 10). Conversely, antibodies against bovine muzzle prekeratin failed to show staining (data not shown).

Antibodies against interstitial collagens and collagen precursors (ie, type I collagen and the aminopeptides of procollagen types I and III) showed similar patterns of staining. There was a fibrillar extracellular staining pattern

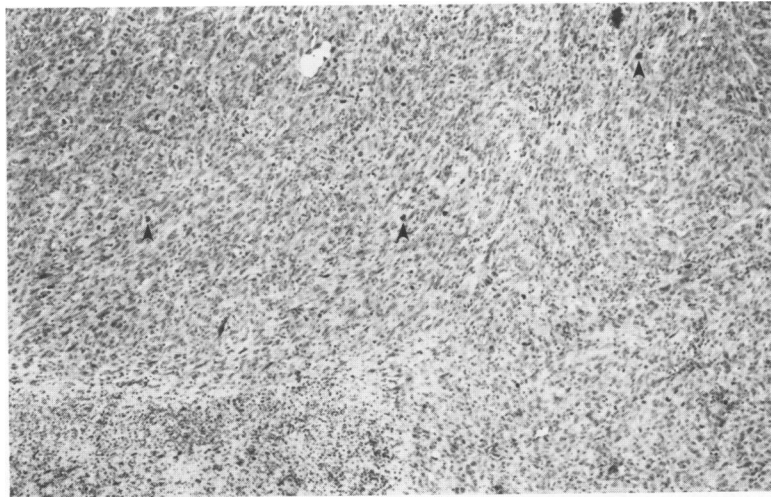


Figure 5. Spindle cell tumor at 37 weeks. There are interlacing bundles of fusiform cells with enlarged hyperchromatic nuclei and numerous mitotic figures (arrowheads). An area of necrosis is visible (lower left) (H&E, X80).

as well as paranuclear (cytosol) staining (Figure 11). The tumor failed to show significant staining with antibodies against basal lamina components (nidogen, type IV-7S collagen), although occasional capillaries were highlighted as circular or elliptical profiles (data not shown).

Electron Microscopy

Electron microscopy of all spindle cell tumors showed similar findings. Two populations of cells were apparent: filiform, fibroblastic cells, and larger, rounded histiocytic cells, with occasional transitional forms between the two (Figure 12).

The fibroblastic cells had long slender cytoplasmic processes and ovoid nuclei with prominent nucleoli. The cytosol contained abundant rough endoplasmic reticulum as well as occasional mitochondria and lysosomal structures. The cell membrane was undulating with scattered pinocytotic vesicles and coated vesicles. These elon-

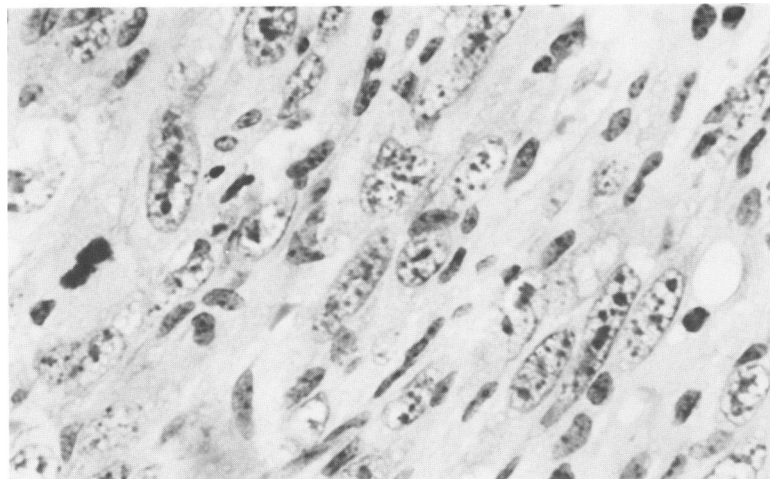
gated cells were frequently closely packed together, but no clear-cut desmosomal complexes were seen. Occasional fine fibrillar material or cross-banded collagen fibers were apparent in the interstices between adjacent cells.

The rounded cells were seen less frequently. Their nuclei were circular or multilobulated with prominent nucleoli, and their cytoplasm contained endoplasmic reticulum, lysosomal structures, and lipid droplets. The cell membrane was more complex, with surface extensions, filopodia, and few surface specializations.

Tissue Culture

Within 1 week of explanting, scattered colonies of cells adhered to the plates. Most of the cells appeared rounded or ameboid and appeared to protrude from the surface of the disk. No syncytia or confluent growth appeared despite long periods of feeding. In the background, occasional

Figure 6. Spindle cell tumor at 37 weeks. The higher power shows the spindle cell area and the striking cytologic atypia (H&E, X800).



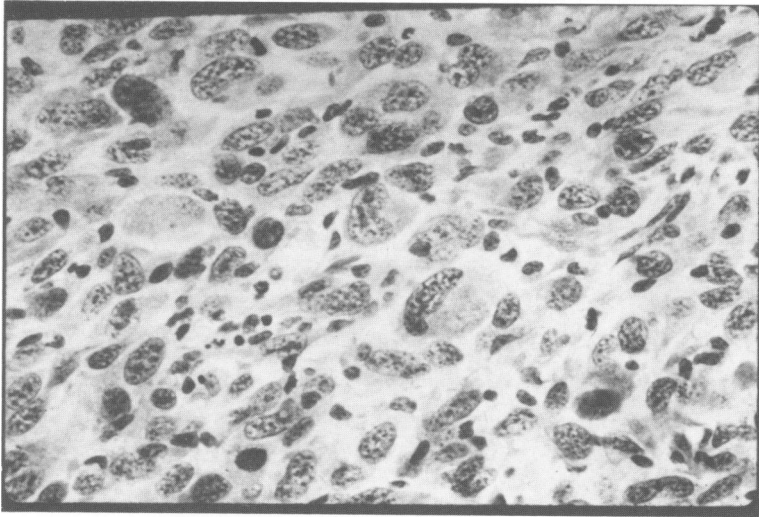


Figure 7. Spindle cell tumor at 37 weeks. Immunoperoxidase for lysozyme clusters of cuboidal histiocytic cells show mild cytoplasmic immunoreactivity (Hematoxylin counterstain, $\times 100$).

fusiform or stellate flattened cells were apparent (Figure 13).

Electron microscopy showed flattened cells and dome-shaped cells, with similar internal structures. Their cytoplasm was filled with numerous primary, secondary, and tertiary lysosomes of varying size and shape. Lamellar golgi complexes and mitochondria were abundant and scattered nonmembrane-bound lipid globules were seen. The nonattached surface showed numerous intermeshing complex filopodia. The nucleus was round or oval and conformed to the overall shape of the cell (Figure 14).

Discussion

The hairless albino mouse is one of the most studied and effective modes of UV light-induced carcinogenesis. Almost all studies of UV-induced neoplasia have concerned

epidermal carcinogenesis rather than dermal carcinogenesis.

It has long been known that certain strains of mice and rats will develop sarcomas or sarcoma-like lesions after UV irradiation. Grady et al²⁶ produced a high percentage of sarcomas in the inner (nonhair-bearing portions) ears of white mice after sufficient UV. Many of these mice developed carcinomas as well, and there were collision tumors between carcinomas and sarcomas. Epstein and Epstein²⁷ produced primarily carcinomas with few sarcomas in hairless mice and primarily sarcomas in hairy albino mice using combinations of UV and dimethyl-benzanthracene. Stenback²⁸ produced sarcomas in shaved Swiss mice by intense short-term treatment with high doses of UV. Few investigators examined these tumors by other than histologic means. In fact, a recent publication indicated that it is not known whether they are of dermal origin.²⁹

Light-microscopic studies of the spindle cell tumors suggested a dermal derivation (Figure 4). Both early le-

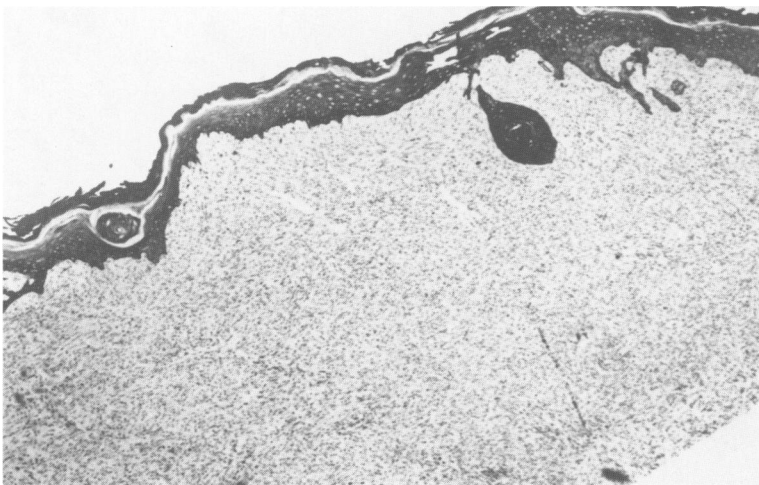


Figure 8. Spindle cell tumor at 34 weeks. Immunoperoxidase for keratin (wide spectrum type). The overlying epidermis shows strong immunoreactivity, whereas the spindle cell tumor fails to stain (Hematoxylin counterstain, $\times 80$).

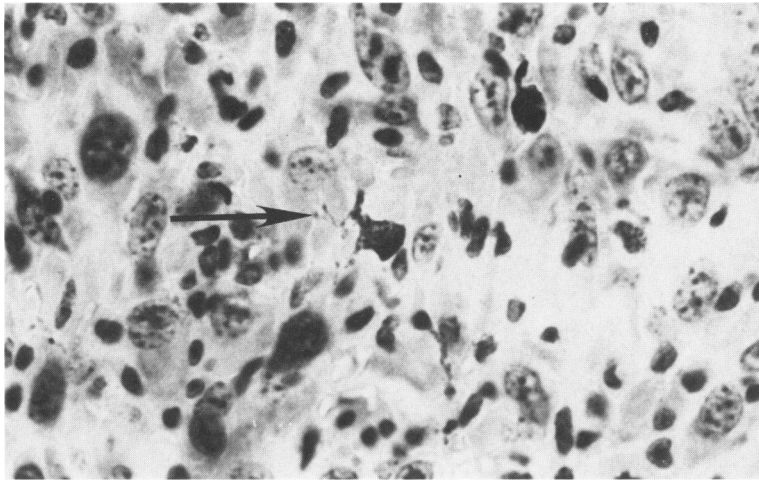


Figure 9. Spindle cell tumor at 37 weeks. Immunoperoxidase for S-100. A probable Langerhans cell with prominent dendrites appears amidst numerous tumor cells (arrow) (Hematoxylin counterstain, $\times 800$).

sions and late lesions showed an expansile dermal nodule. Despite adjacent, normal, or dysplastic epidermis, multiple sections failed to disclose evidence of an epidermal origin, or a merging with epidermis. This contrasts with studies of human sarcomatous squamous cell carcinomas, in which an epidermal derivation can often be established.^{7,30}

Electron microscopy of the tumors (Figure 12) (large or small, or early or late in the photocarcinogenic regimen) further defined these changes. There were exclusively mesenchymal cells: long, slender, fibroblastic cells and histiocytic cells, as well as intermediate forms. Other features, such as the amount of extracellular matrix or filamentous material in the cytosol, varied from section to section or tumor to tumor. Unequivocal evidence of epithelial or melanocytic differentiation (ie, intercellular junctions, tonofilaments, or melanosomes) was not seen.

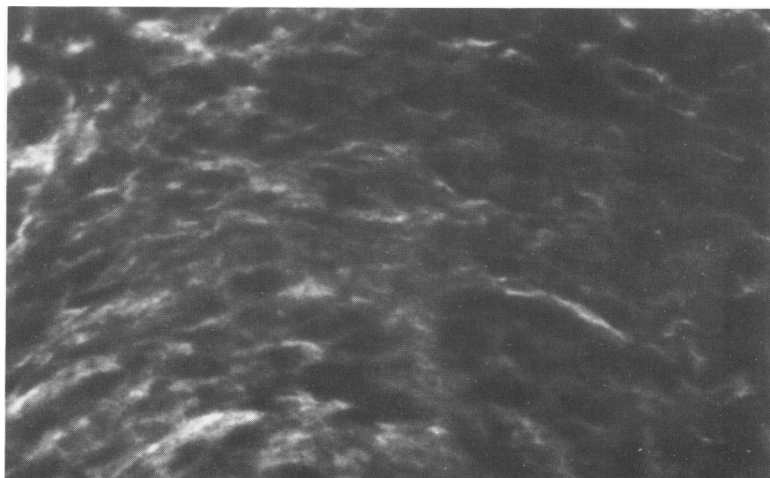
The immunochemical studies, particularly those using anti-intermediate filament antibodies, further supported mesenchymal differentiation. The tumors were repeatedly

negative for both wide spectrum keratin and epidermally derived keratin (Figure 8). The former antibodies are directed against multiple, low molecular weight keratin species, which are present in diverse epithelia of the body, including all adnexa.¹⁹ The latter have a much more restricted distribution in squamous epithelia.^{18,31}

Although the absence of keratin effectively excludes epithelial differentiation, it is theoretically possible that, in reversion to a mesenchymal phenotype, epithelia lose or reduce expression of keratin. In actual practice, however, this occurs infrequently. Most spindle squamous cell carcinomas or spindle cell epithelial sarcomas contain abundant or focal keratin.³¹ This persistence of expression of keratin in diverse cell types despite malignant conversion or phenotypic transformation makes keratin extremely sensitive and specific as a marker for epithelial differentiation.

Vimentin, on the other hand, is much less specific, and is normally present in diverse mesenchymal cell types, including lymphoid cells, fibroblasts, smooth muscle

Figure 10. Spindle cell tumor at 37 weeks. Immunofluorescence for vimentin. There is strong intracytoplasmic staining contrasting with centrally unstained nucleus ($\times 400$).



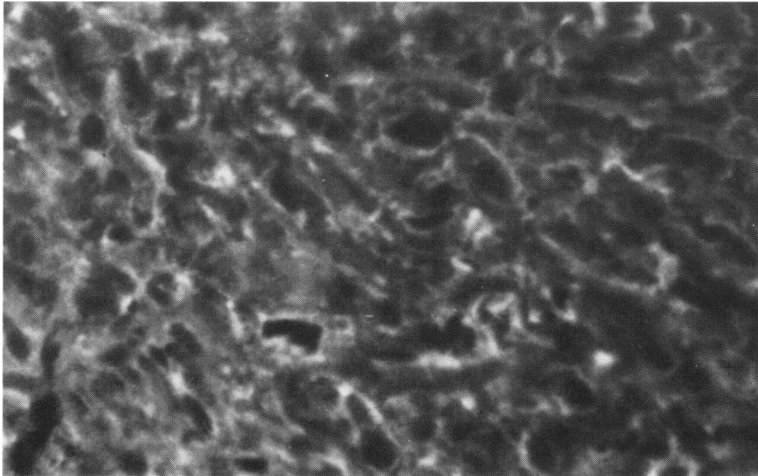


Figure 11. Spindle cell tumor at 37 weeks. Immunofluorescence for type I collagen. There is strong intracytoplasmic staining and fibrillar extracellular staining ($\times 400$).

cells, endothelium, melanocytes, and histiocytes. It frequently is also coexpressed with other intermediate filament types.³² In many tumors (eg, synovial sarcoma and epithelioid sarcoma), in tissue culture, or during changes of organogenesis, vimentin may be expressed simultaneously or consecutively with other intermediate filament types.³¹ Its abundance in the UV-induced tumor (Figure 10) is consistent with mesenchymal derivation, and in conjunction with the absence of keratin allows it to be categorized as probably mesenchymally derived.

The morphologic electron microscopic and immunocytochemical features of these tumors revealed a phenotypic heterogeneity within the tumor with both fibrocytic and histiocytic differentiation.

By light and electron microscopy, there appeared to be two populations of cells: slender, fusiform cells (Figure 6) and round cuboidal cells (Figure 7). From field to field, the proportion of each cell type varied, and sometimes one merged imperceptibly into the other. Neither cell type appeared to form discrete patterns, although sometimes

the spindle cells formed irregular fascicles (Figure 5). The degree of cytologic atypia and the number of mitotic figures were striking.

Electron microscopy demonstrated that the former population of spindle cells had features of fibrocytes. The cells were fusiform, with ovoid nuclei. They possessed long cytoplasmic processes, had abundant rough endoplasmic reticulum, and had a smooth cell membrane. The rounder cells, on the other hand, frequently had less endoplasmic reticulum, a more undulating cell membrane, lipid droplets, and lysosomal structures, with features more typical of histiocytes. Sometimes cells were observed that showed features of both types (Figure 12).

Morphologic studies of human atypical fibroxanthoma have yielded similar findings. Fibroblast-like cells are admixed haphazardly with rounded cells. Atypia, pleomorphism, and mitotic figures are abundant. No organoid pattern is apparent. Electron-microscopic studies have also shown similar features: a mixed population of fibrocytes and lipid-laden histiocytes, with transitional forms be-

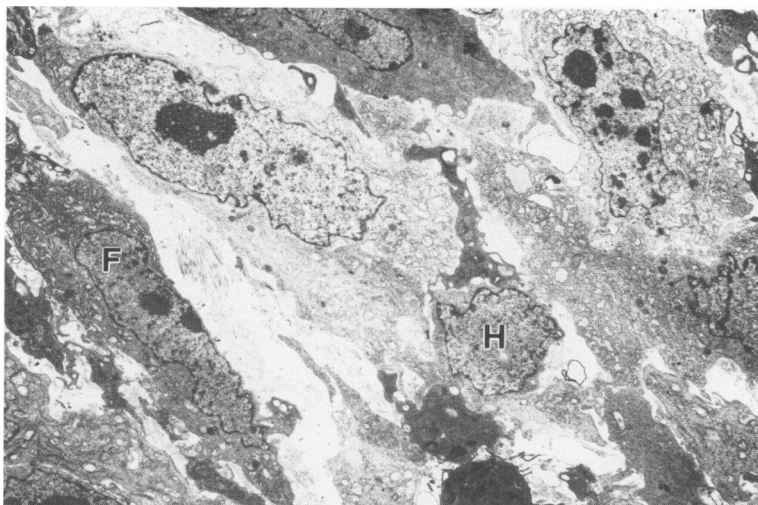


Figure 12. Electron microscopy spindle cell tumor at 34 weeks. Irregularly shaped fibroblastlike (F) cells are adjacent to rounded histiocytic (H) cells. Abundant intercellular fibrillar matrix is apparent. Note the abundant organelles: rough endoplasmic reticulum, golgi, lipid droplets, and lysosomes. No intercellular nexi or premelanosomes are evident (uranyl acetate and lead citrate, $\times 3640$).

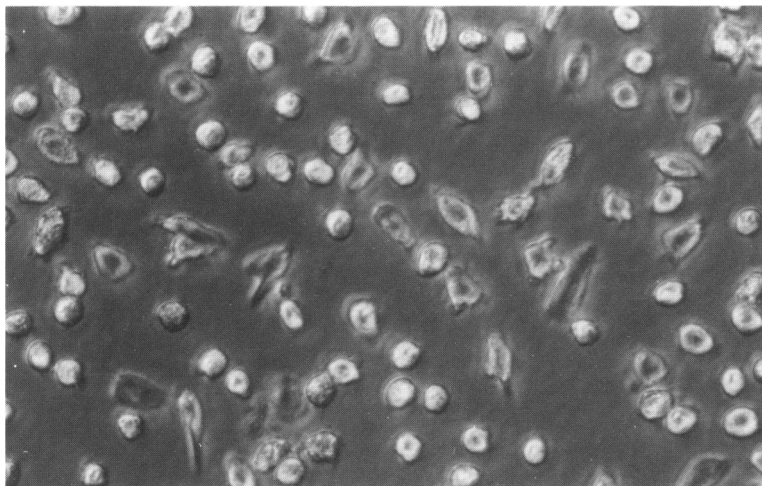


Figure 13. *Tissue culture spindle cell tumor at 37 weeks (after 4 weeks of growth). Note the irregular dispersed colony with dome shaped cells, and scattered, flattened polygonal cells.*

tween the two.⁹ Some investigators have also found myofibroblasts,⁸ and others have found cells with Birbeck granules.^{10,12} However, evidence of epithelial or melanocytic differentiation was not detected. This range of differentiation has led some to suggest that atypical fibroxanthoma is not necessarily a homogeneous entity but possesses phenotypic heterogeneity.

In the mouse tumors studied, there was both intracytoplasmic and extracellular staining for procollagens I and III and for type I collagen (Figure 11). The antibodies against the procollagens recognize a portion of the amino terminal peptide, whereas the antibodies directed against mature type I collagen recognize the helical domain.³³ These antigens may be present intracellularly and in the extracellular matrix.³⁴

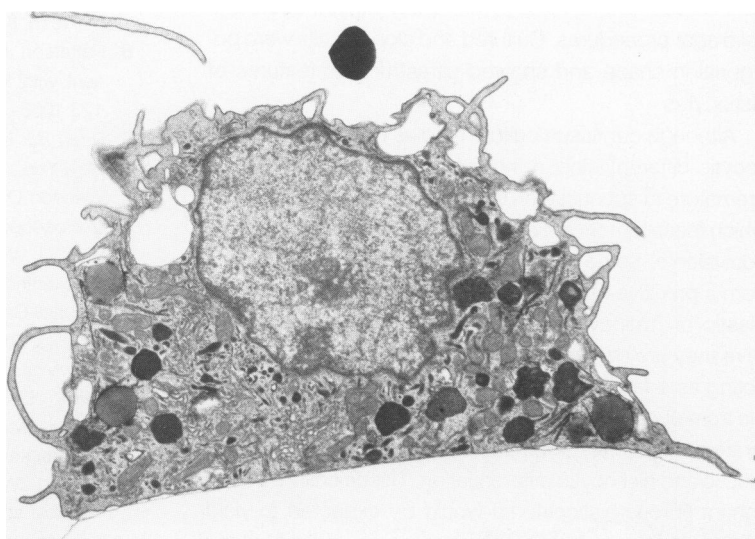
The presence of such intense staining within the cells and in the matrix is expected in a tumor that is actively producing extracellular matrix. This further confirms its

partial fibrocytic differentiation, as only a few nonepithelial cell types, fibrocytes, leiomyocytes, and Schwann cells, produce this much collagen.³⁵ The absence of significant basal lamina staining militates against a Schwann cell or leiomyocyte origin and further supports a fibrohistiocytic origin.³⁶

Few investigators have studied the distribution of collagen types in fibrohistiocytic neoplasms. Hall et al³⁷ examined the distribution of interstitial and basal lamina collagens in a fibrosarcoma and found primarily extracellular type I and type V collagens. Roholl et al³⁸ discovered primarily type III collagen and less type I collagen in two malignant fibrous histiocytomas. Collagen production would be anticipated in the fibroblast-like areas of atypical fibroxanthoma.

The histiocytic markers, α_1 -anti-trypsin and lysozyme (Figure 7), were variably present. Alpha-1-anti-trypsin is a characteristic marker for malignant neoplasms with al-

Figure 14. *Electron microscopy tissue culture of Figure 13, having an ovoid cell, has prominent filopodia, and oval nucleus. Numerous lipid globules and lysosome structures are evident (uranyl acetate and lead citrate, $\times 7000$).*



leged histiocytic differentiation, whereas lysozyme is a better marker for reactive histiocytic proliferations.³⁹ As the expression of these markers can be variable from tumor to tumor and as these tumors showed more spindle cell foci, this limited expression would be anticipated. Similar variable distribution has been observed in human atypical fibroxanthoma.¹⁴

The presence of numerous S-100 positive dendritic cells has been observed repeatedly in human atypical fibroxanthoma¹⁴ and in the mouse tumors (Figure 9). At first, on the basis of electron microscopy, it was proposed that atypical fibroxanthoma may be in part a Langerhans cell proliferation. It is now believed that the Langerhans cell component is just an admixed immigrant population, which can comprise from 5% to 30% of the cells present.¹⁵

Initial attempts to establish a cell line in the mouse tumor were largely unsuccessful. Rather, multiple explants of tumor tissue produced isolated colonies with only limited potential for growth. Each colony showed a distinctive and identical morphology: dome-shaped, amoeboid cells, with peripheral flattened polygonal cells (Figure 13). Electron microscopy demonstrated evidence of primarily histiocytic differentiation in all cell types (Figure 14).

To our knowledge, there has been no successful culture of human atypical fibroxanthomas. Several investigators, however, have cultured malignant fibrous histiocytomas. Roholl et al,³⁸ using a similar explant technique, produced two cell lines from two deep malignant fibrous histiocytomas. Cultures from one tumor showed clusters of cells with rounded and triangular forms and cultures from the other showed more confluent growth with more elongate forms. Electron microscopy of the former culture showed primitive mesenchymal cells with few identifying features and of the latter more fibroblastic differentiation. Shirasuna et al⁴⁰ cultured and cloned a maxillary malignant fibrous histiocytoma (MFH) using explant and semi-solid agar procedures. Cultured and cloned cells were polygonal in shape and showed ultrastructural features of histiocytes.

Although our tissue culture studies demonstrated histiocytic differentiation in the mouse tumor, we think it is premature to speculate on the precise origin of the cells of which these tumors are composed or those in their human equivalents. Some investigators believe they are derived from a primitive mesenchymal cell with capacity for fibroblastic or histiocytic differentiation, whereas others believe they are derived from a tissue histiocyte capable of acting as a facultative fibroblast. No conclusion is possible from our study or from those of others, but in all tumors examined thus far there has been evidence of both fibroblastic and histiocytic differentiation. Tissue culture of malignant fibrous histiocytoma would be expected to yield findings similar to atypical fibroxanthoma. Indeed, many

investigators currently believe atypical fibroxanthoma, is a superficial, low grade malignant fibrous histiocytoma.⁴¹

We believe that the more appropriate term for the neoplasm produced in these animals is atypical fibroxanthoma, or malignant fibrous histiocytoma, rather than sarcoma or fibrosarcoma. This change in nomenclature rests primarily on the observation, repeatedly confirmed by light microscopy, electron microscopy, and immunocytochemistry, that this tumor shows fibrohistiocytic differentiation. The features correspond to the current description of atypical fibrohistiocytic neoplasia. Fibrosarcoma is now considered a relatively rare neoplasm that shows only a fibroblastic mode of differentiation, with a herringbone pattern and limited cytologic atypia.⁴¹

The unequivocal demonstration of ultraviolet-induced dermal neoplasia now leads to an interesting experimental model. Questions can be asked regarding dosage effects, co-initiators, promoters, and the relative contributions of different spectra of ultraviolet irradiation that would have considerable clinical relevance.

References

1. Kempson RL, McGavran MH: Atypical fibroxanthomas of the skin. *Cancer* 1964, 17:1463-1471
2. Kroe DJ, Pitcock JA: Atypical fibroxanthoma of the skin: Report of ten cases. *Am J Clin Pathol* 1969, 51:487-492
3. Fretzin DF, Helwig EB: Atypical fibroxanthoma of the skin. A clinico-pathologic study of 140 cases. *Cancer* 1973, 31:1541-1552
4. Starink TM, Hausman R, Delden LV, Neering H: Atypical fibroxanthoma of the skin. Presentation of 5 cases and a review of the literature. *Br J Dermatol* 1977, 97:167-177
5. Dahl I: Atypical fibroxanthoma of the skin: A clinico-pathological study of 57 cases. *Acta Pathol Microbiol Immunol Scand [A]* 1976, 84:183-197
6. Patterson JW, Jordan WP: Atypical fibroxanthoma in a patient with xeroderma pigmentosum. *Arch Dermatol* 1987, 123:1066-1070
7. Reed RJ: New concepts in surgical pathology of the skin. New York, Wiley Biomedical 1976
8. Weedon D, Kerr JFR: Atypical fibroxanthoma: An electron microscope study. *Pathology* 1975, 7:173-177
9. Barr RJ, Wuerker RB, Graham JH: Ultrastructure of atypical fibroxanthoma. *Cancer* 1977, 40:736-743
10. Alguacil-Garcia A, Unni KK, Goellner JR, Winkelmann RK: Atypical fibroxanthoma of the skin: An ultrastructural study of two cases. *Cancer* 1977, 40:1471-1480
11. Kemp JD, Stennk S, Arons M, Fischer J et al: Metastasizing atypical fibroxanthoma: Co-existence with chronic lymphocytic leukemia. *Arch Dermatol* 1978, 114:1533-1535
12. Carson JW, Schwartz RA, McCandless CM, French SW: Atypical fibroxanthoma of the skin: Report of a case with Langerhans-like granules. *Arch Dermatol* 1984, 120:230-239

13. Glavin FL, Cornwell ML: Atypical fibroxanthoma of the skin metastatic to a lung. Report of a case: Features by conventional and electron microscopy, and a review of relevant literature. *Am J Dermatopathol* 1985, 7:57-63
14. Leong AS, Milios J: Atypical fibroxanthoma of the skin: A clinicopathologic and an immunohistochemical study. A Discussion of its Histogenesis. *Histopathology* 1987, 11:463-475
15. Ricci A, Cartun RW, Zakowski MF: Atypical fibroxanthoma: A study of 14 cases emphasizing the presence of Langerhans' histiocytes with implications for differential diagnosis by antibody panels. *Am J Surg Pathol* 1988, 12:591-598
16. Epstein JH: Photocarcinogenesis: A review. *NCI Monogr* 1978, 50:13-25
17. Epstein JH: Photocarcinogenesis, skin cancer, and aging. *J Am Acad Dermatol* 1983, 9:487-502
18. Schlegel R, Banks-Schlegel S, McLeod JA, Pinkus GS: Immunoperoxidase localization of keratin in human neoplasms: A preliminary survey. *Am J Pathol* 1980, 101:41-50
19. Franke WW, Weber K, Osborn M, Schmid E, Freudenstein C: Antibody to prekeratin: Decoration of tonofilament-like arrays in various cells of epithelial character. *Exp Cell Res* 1978, 116:429-445
20. Franke WW, Schmid E, Winter S, Osborn M, Weber K: Widespread occurrence of intermediate-sized filaments of the vimentin-type in cultured cells from diverse vertebrates. *Exp Cell Res* 1979, 123:25-46
21. Nowack H, Gay S, Wick G, Becker U, Timpl R et al: Preparation and use in immunohistology of antibodies specific for type I and type III collagen and procollagen. *J Immunol Methods* 1976, 12:117-24
22. Timpl R, Dziadek M, Fujiwara S, Nowack H, Wick G: Nidogen: A new self-aggregating basement membrane protein. *Eur J Biochem* 1983, 137:455-65
23. Risteli J, Wick G, Timpl R: Immunological characterization of the 7S domain of type IV collagen. *Coll Relat Res* 1981, 1: 419-432
24. Hsu SM, Raine L, Fanger H. Use of avidin-biotin peroxidase complex (ABC) in immunoperox techniques. *J Histochem Cytochem* 1981, 29:577-580
25. Phelps RG, Martinez-Hernandez A, Goldberg BD: Ultrastructural immunocytochemical localization of type I procollagen in cultured human fibroblasts. *Collagen Rel Res* 1985, 5: 405-414
26. Grady HG, Blum HF, Kirby-Smith JS: Pathology of tumors of the external ear in mice induced by ultraviolet radiation. *JNCI* 1941, 2:269-276
27. Epstein JH, Epstein WL: A study of tumor types produced by ultraviolet light in hairless and hairy mice. *J Invest Dermatol* 1963, 41:463-473
28. Stenback F: Life history and histopathology of ultraviolet light-induced skin tumors. *NCI Monogr* 1978, 50:57-70
29. Kligman LH, Kligman AM: Histogenesis and progression of ultraviolet light-induced tumors in hairless mice. *JNCI* 1981, 67:1289-1297
30. Evans HL, Smith JL Jr. Spindle cell squamous carcinomas and sarcoma-like tumors of the skin: A comparative study of 38 cases. *Cancer* 1980, 45:2687-2697
31. Battiforah H: Clinical applications of the immunohistochemistry of filamentous proteins. *Am J Surg Pathol* 1988, 12(Suppl 1):24-42
32. Nagle RB: Intermediate Filaments: A review of the basic biology. *Am J Surg Pathol* 1988, 12(Suppl 1):4-16
33. Pesciotta DM, Olsen BR: The Cell Biology of Collagen Secretion In *Immunocytochemistry of the Extracellular Matrix*, Ed. Furthmayr H, vol. II., Bold Raton, Florida, CRC Press 1982, pp 1-18
34. Fleischmajer R, Timpl R, Tuderman L, Raisher L, Wiestner M, Perlish JS, Graves PN et al: Ultrastructural identification extension of aminoproteptides of type I and type III collagens in human skin. *Proc Natl Acad Sci USA* 1981, 78:7360-7364
35. Furthmayr H, Von der Mark K: The use of antibodies to connective tissue proteins in studies on their localization in tissues, *Immunocytochemistry of the Extracellular Matrix*, Ed. Furthmayr H, vol. II, Bold Raton, Florida, CRC Press 1982, pp 89-117
36. Roholl PJM, DeJong ASH, Ramaekers FCS: Review: Application of markers in the diagnosis of soft tissue tumors. *Histopathology* 1985, 9:1019-1035
37. Hall J, Tseng SCG, Timpl R, Hendrix MJC, Stern R: Collagen types in fibrosarcoma: Absence of type III collagen in reticulins. *Hum Pathol* 1985, 16:439-446
38. Roholl PJM, Kleyne J, Van Blokland M, Spies PL, Rutgers DH, Albus-Lutter CE, Van Unnik JAM et al: Characterization of two cell lines derived from two malignant fibrous histiocytomas. *J Pathol* 1986, 150:103-112
39. Nemes Z, Thomazy V: Factor XIIIa and the classic histiocytic markers in malignant fibrous histiocytoma: A comparative immunohistochemical study. *Hum Pathol* 1988, 19:822-829
40. Shirasuna K, Sugiyama M, Miyazaki T: Establishment and characterization of neoplastic cells from a malignant fibrous histiocytoma: A possible stem cell line. *Cancer* 1985, 55: 2521-2532
41. Enzinger FM, Weiss SW: *Soft Tissue Tumors*, 2nd ed. St. Louis, C. V. Mosby Co. 1988. pp. 201-222, 269-273

Acknowledgment

We thank Drs. Fasy and Burstein for reviewing the manuscript and Ms. Rebecca Carandang for her expert secretarial assistance.